Available online at www.sciencedirect.com

SciVerse ScienceDirect

Ceramics International 39 (2013) S273–S276

CERAMICS INTERNATIONAL

www.elsevier.com/locate/ceramint

First principles calculations of Hydrogen—Titanium vacancy complexes in $SrTiO_3$

Ittipon Fongkaew[a,b], Jiraroj T-Thienprasert[b,c], D.J. Singh[d], M.-H. Du[d], Sukit Limpijumnong[a,b,*]

[a]School of Physics, Suranaree University of Technology, Nakhon Ratchasima 30000, Thailand
[b]Thailand Center of Excellence in Physics (ThEP Center), Commission on Higher Education, Bangkok 10400, Thailand
[c]Department of Physics, Faculty of Science, Kasetsart University, Bangkok 10900, Thailand
[d]Oak Ridge National Laboratory, Oak Ridge, TN 37831, USA

Available online 16 October 2012

Abstract

Hydrogen has been reported to serve exclusively as a donor in many oxides, including $SrTiO_3$. In a perfect crystal, a proton stays near an O atom, forming a strong O–H bond. In the presence of cation vacancies, i.e., Sr vacancy and Ti vacancy, protons prefer to electrically passivate the cation vacancies by forming strong bonds with the O atoms surrounding the vacancy. These result in the formation of nH–V_{Sr} and nH–V_{Ti} complexes. Based on first principles density functional calculations, local configurations and vibration signatures of nH–V_{Sr} complexes and their vibrational signatures have been previously reported [T-Thienprasert et al., Identification of hydrogen defects in $SrTiO_3$ by first-principles local vibration mode calculations, Physical Review B 85, 125205 (2012)]. Here, we report the computational results for nH–V_{Ti} complexes and compare the results with infrared measurements reported in the literatures.

Keywords: $SrTiO_3$; Hydrogen; Vacancy; First principles calculations

1. Introduction

Hydrogen (H) is known to be an abundant impurity, which can affect materials' electronic properties [1–4]. In most oxide materials, H acts exclusively as a donor and prefers to stay close to oxygen atoms, forming strong O–H bonds. These O–H bonds can be considered as oscillators with distinct natural stretch mode frequencies of about 3000 cm^{-1} that can be directly observed by infrared (IR) measurements.

Strontium titanate ($SrTiO_3$) is one of the most important oxide materials because of its potential to be used in dielectric and optical devices [5–8], as well as its potential to be used as a substrate for superconducting thin films [9]. $SrTiO_3$ has a cubic perovskite structure at room temperature and a tetragonal structure at the temperature below 105 K [10]. In 1980, based on polarized IR absorption measurement, Weber and Kapphan (WK) observed the vibration band at ~3500 cm^{-1} [11,12]. They also studied the effects of uniaxial stress and electric field on the vibration band. Later, polarized Raman scattering measurement was carried out by the same group [13]. At room temperature, WK found the main peak centered at 3495 cm^{-1} accompanied with small peaks in the range of 3505–3520 cm^{-1}. WK proposed that the frequencies belong to a single H interstitial in $SrTiO_3$. Recently, Tarun and McCluskey [14] (TM) experimentally observed additional double peaks centered at 3355 and 3384 cm^{-1}. They assigned these local vibrational modes to a complex defect between a Sr vacancy and two H atoms (2H–V_{Sr}).

Recently, based on first principles calculations, we have revealed that H interstitial has a vibrational frequency far lower than 3500 cm^{-1} [15]. We also showed that one or two interstitial H atom(s) could be trapped by V_{Sr} forming nH–V_{Sr} complexes (n=1 or 2). In the complexes, H atoms form strong O–H bonds with the O atoms surrounding V_{Sr}

*Corresponding author at: School of Physics, Suranaree University of Technology, Nakhon Ratchasima 30000, Thailand. Tel.: +66 44 22 4319; fax: +66 44 22 4185.
E-mail address: sukit@sut.ac.th (S. Limpijumnong).

0272-8842/$ - see front matter © 2012 Elsevier Ltd and Techna Group S.r.l. All rights reserved.
http://dx.doi.org/10.1016/j.ceramint.2012.10.076

in the direction pointing toward the vacancy center. As we obtained the calculated vibrational frequencies of nH–V_{Sr} complexes very close to the observed peaks ($\sim$3500 cm^{-1}) by WK with consistent oscillator directions, we identified WK's observation to be nH–V_{Sr} complexes; not a single H interstitial [15]. For the double peaks centered at 3355 and 3384 cm^{-1} observed by TM, we previously discussed that they could not arise from 2H–V_{Sr} complexes as proposed by TM because the frequencies were not in agreement and the complexes could not explain the coupling observed experimentally. In the same article [15], we proposed that the double peaks that TM observed may belong to H and Ti vacancy complexes nH–V_{Ti} but we did not provide the results in detail. In this paper, we report the binding energies, local structures and the detailed vibrational frequencies of complex defects between H and V_{Ti} based on first-principles density functional calculations. We show that the vibrational frequencies observed by TM are consistent with nH–V_{Ti} complexes.

2. Computational method

In this work, first-principles density functional theory (DFT) within the local density approximation (LDA) was used. To describe the electron-ion interactions, the projector-augmented wave (PAW) method with ultrasoft pseudo potentials, as implemented in VASP code, was used [16–18]. The cutoff energy for the plane wave basis set was set at 500 eV. We obtained the calculated lattice constant of cubic $SrTiO_3$ of 3.87 Å which is in good agreement with the experimental value of 3.905 Å [19]. To study defects in $SrTiO_3$, a supercell approach with a supercell size of 135 atoms, which is a $3\times3\times3$ repetition of cubic-perovskite unit cell, was used [20]. For k-space integration, Monkhorst–Pack scheme with a shifted $2\times2\times2$ k-point sampling was employed. For charged defects, a jellium background is used to suppress the long-range Coulombic interactions between supercells. All atoms were allowed to relax until the residue (Hellmann–Feynman) forces [21] become less than 10^{-3} eV/Å.

Following the description of the binding energy between a Sr vacancy and H interstitial described in Ref. [15], the binding energy between a Ti vacancy (V_{Ti}^{4-}) and H interstitial, or simply a proton, (H^+) and between $(n\text{H}–V_{Ti})^{-4+n}$ and a proton can be defined as

$$\Delta E = E_{tot}(\text{H}–V_{Ti})^{3-} + E_{tot}(\text{bulk}) - E_{tot}\left(V_{Ti}^{4-}\right) - E_{tot}\left(\text{H}^+\right) \quad (1)$$

and

$$\Delta E = E_{tot}([n+1]\text{H}–V_{Ti})^{-3+n} + E_{tot}(\text{bulk}) - E_{tot}(n\text{H}–V_{Ti})^{-4+n} - E_{tot}\left(\text{H}^+\right) \quad (2)$$

where $E_{tot}(\beta)$ is the total energy of a supercell containing the complex (or impurity) β.

Eq. (1) describes the binding energy of the reactions

$$V_{Ti}^{4-} + \text{H}^+ \rightarrow (H–V_{Ti})^{3-} \quad (3)$$

which is the energy gain when a proton is bound in a V_{Ti}^{4-}. Eq. (2) is a more general case describing the binding energy of an addition proton to the existing $(n\text{H}–V_{Ti})^{-4+n}$ complex (n=0, 1, 2, 3). Note that, Eq. (1) is a specific case of Eq. (2) when n=0.

3. Results and discussion

3.1. Binding energies

In this work, we focus our attentions to H and Ti vacancy complex defects. Under n-type conditions, V_{Sr} and V_{Ti} are double and quad acceptors, respectively. At low temperature, an interstitial H is always a single donor (or simply a proton) binding strongly to one of the O atoms in STO with the lowest-energy configuration called "OA" [15]. However, the interstitial H is not very stable. It can be annealed out of the STO crystals at even below room temperature ($\sim$100 K) [15], and it has frequency of only $\sim$2700 cm^{-1}. Consequently, we proposed that the O–H oscillators observed in many IR experiments, with the frequency range of 3300–3500 cm^{-1} [10–14,22], are more likely associated with H complex defects.

For H and V_{Sr}, V_{Sr} in charge state 2 (V_{Sr}^{2-}) could trap a proton (H^+) to form $(\text{H}–V_{Sr})^{\tilde{}}$ complex defect with a reasonably large binding energy of 0.84 eV [15]. The $(\text{H}–V_{Sr})^{\tilde{}}$ complexes defect could further bind another proton to form a neutral 2H–V_{Sr} complex defects. In Ref. [15], we have studied in detail of the possible configurations and found two most stable 2H–V_{Sr} complexes with the binding energy of the second proton of 0.81 and 0.79 eV, respectively.

For H and V_{Ti}, V_{Ti} in charge state 4(V_{Ti}^{4-}), it can trap up to four protons to form a nH–V_{Ti} complex defect. V_{Ti}^{4-} traps the first proton to form $(\text{H}–V_{Ti})^{3}$ with a large binding energy of $\sim$1.94 eV. The $(\text{H}–V_{Ti})^{3}$ could trap another proton to form a $(2\text{H}–V_{Ti})^{2}$ complex defect with a binding energy for the second proton of 1.62 eV. In this case, there are two possible ways to add the second proton to form a $(2\text{H}–V_{Ti})^{2-}$ complex defect. (1) The second proton is attached to the O atom on the opposite side of the vacancy from the O atom attached by the first proton. (2) The second proton is attached to one of the four O atoms that are the neighbor of the vacancy and sits next to the O atom attached by the first proton. The two configurations are relaxed at two minimum energy configurations as illustrated in Fig. 2 (point c and d). To determine the energy barrier between the two configurations, we employed the climbing image nudged elastic band method (NEB) [23–26].

In Fig. 2, the highest energy structure (point a) is when the two O–H bonds are pointing directly at each other. To reduce the dipole-dipole interactions, the two O–H bonds are tilted off the equilibrium position into point b, lowering the energy by about 0.05 eV. Without any barrier, the O–H bonds can further tilt into point c, lowering the energy by another 0.05 eV. The structure at point c is the local minimum-energy structure for the first configuration. Next, if we force one of the protons to break its O–H bond and move to form a bond with another O atom, we obtained the

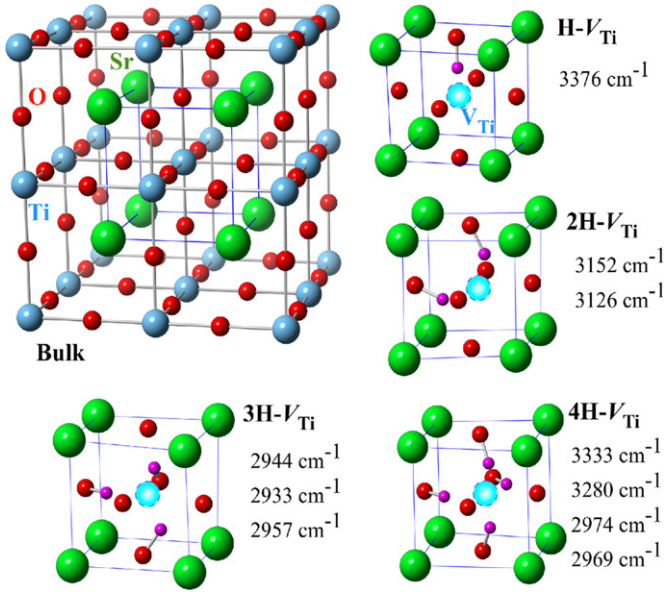

Fig. 1. The local structures of bulk $SrTiO_3$ and H–V_{Ti}, 2H–V_{Ti}, 3H–V_{Ti}, and 4H–V_{Ti} complexes. Green, blue, red, and pink spheres represent the Sr, Ti, O, and H atoms, respectively. The stretch vibrational frequencies for each configuration are also shown. (For interpretation of the references to color in this figure legend, the reader is reffered to the web version of this article.)

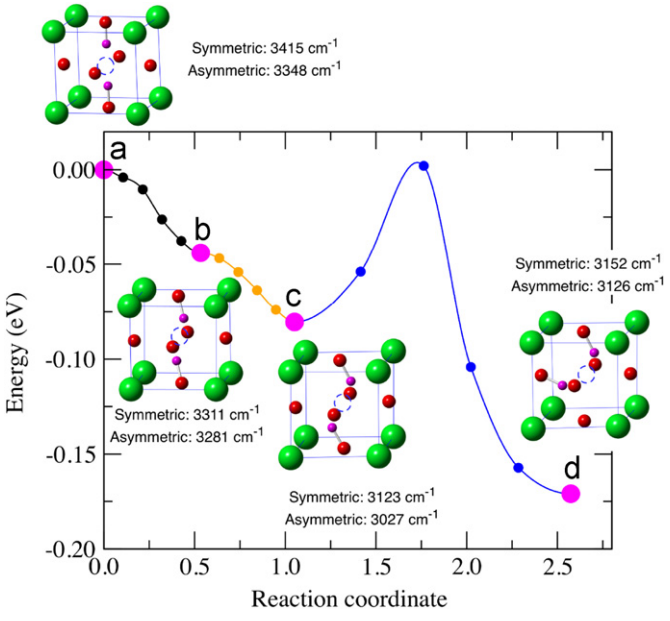

Fig. 2. Illustration of the energy path relating different configurations of $(2H–V_{Ti})^2$ complexes obtained from the nudged elastic band method. Points (a)–(d) indicate interesting configurations of which the configurations at (c) and (d) are the local minimum and global minimum energy configurations, respectively. The stretch vibrational frequencies are also listed for each configuration. (For interpretation of the references to color in this figure legend, the reader is reffered to the web version of this article.)

$c \rightarrow d$ path with a small energy barrier of $\sim$0.1 eV for the proton to move from the first configuration to the lower energy (second) configuration, as shown in Fig. 2. This rather low energy barrier indicates that protons in the V_{Ti} could move rather freely to find their global minimum energy positions. Therefore, majority of the $(2H–V_{Ti})^{2-}$ complexes should exist in their lowest energy configuration (point d) at reasonably low temperatures.

The $(2H–V_{Ti})^{2-}$ complexes could trap another proton to form $(3H–V_{Ti})^{-}$ complexes There are two possible configurations for the $(3H–V_{Ti})^{-}$ complexes with the lower energy one shown in Fig. 1. The $(3H–V_{Ti})^{-}$ complexes could further bind with another proton to form neutral 4H–V_{Ti} complexes. Again, there are two possible configurations for the 4H–V_{Ti} complexes with the lower energy one shown in Fig. 1. The formation of these complexes can be summarized in the following reaction equations.

$$
\begin{aligned}
&H^{1+} + V_{Ti}^{4-} \rightarrow (H - V_{Ti})^{3-} + 1.94\ \text{eV},\\
&H^{1+} + (H - V_{Ti})^{3-} \rightarrow (2H - V_{Ti})^{2-} + 1.62\ \text{eV},\\
&H^{1+} (2H - V_{Ti})^{2-} \rightarrow (3H - V_{Ti})^{-} + 1.51\ \text{eV},\\
&H^{1+} + (3H - V_{Ti})^{-} \rightarrow (4H - V_{Ti}) + 1.00\ \text{eV}
\end{aligned}
\qquad (6)
$$

3.2. Local vibrational frequencies of complex defects

The vibrational frequency associated with each defect was determined by calculating the dynamical matrix based on the harmonic approximations as described in Ref. [27] To test the reliability of the calculations, we first calculated the vibrational modes of a water molecule and obtained the vibrational frequencies of 3712, 3825, and 1533 cm^{-1} for symmetric stretching, asymmetric stretching, and bending modes, respectively. Comparing with the experimental values of 3657, 3756, and 1595 cm^{-1} [28,29] the computational values contain the error bar of $\sim$70 cm^{-1}.

Next, we calculated the vibration signatures of nH–V_{Ti} complex defects. We found that all nH–V_{Ti} complexes give the vibrational frequency below 3400 cm^{-1} (see Fig. 1). The $(H–V_{Ti})^{3-}$ complex has the calculated vibrational frequency of 3376 cm^{-1} in a reasonable agreement with the values observed by TM. When a second proton is added to form $(2H–V_{Ti})^{2-}$ complex, the two O–H bonds can vibrate as two oscillators. We found that, unlike the case of 2H–V_{Sr} that the two oscillators have no coupling between them [15], here there is a coupling between the two oscillators. The reason can be attributed to the closer distance of the two oscillators in the case of the $(2H–V_{Ti})^{2-}$ complex compared to the 2H–V_{Sr} complex. The vibrational frequency of the $(2H–V_{Ti})^{2-}$ complex is split into two values, as shown in Fig. 1. Interestingly, the two calculated frequencies are differed by 26 cm^{-1}, which is in a good agreement with the splitting of the two peaks of 29 cm^{-1} observed by TM [14]. This is the strongest indication that the observed IR absorption peaks by TM at 3355 and 3384 cm^{-1} should come from $(2H–V_{Ti})^{2-}$ complex rather than 2H–V_{Sr} complex. Note, however, that the absolute values of the calculated vibrational frequencies of the $(2H–V_{Ti})^{2-}$ complex are only 3152 and 3126 cm^{-1}, somewhat lower than the values observed by TM (by about 7%). In addition to the vibrational frequencies of the lowest energy configuration, those of the higher energy configurations have also been

calculated and are shown in Fig. 2. Beside the vibration frequencies of $(H–V_{Ti})^{3-}$ and $(2H–V_{Ti})^{2-}$ complexes, we further calculated the vibration of $(3H–V_{Ti})^{-}$ and $4H–V_{Ti}$ complexes in their lowest-energy configurations and showed their vibrational frequencies in Fig. 1. We found all calculated vibrational frequencies to be in the range of 2900–3400 cm^{-1}.

4. Conclusion

Based on first-principles density functional calculations, we reported the detailed study of complex defects between H and Ti vacancy ($nH–V_{Ti}$ complexes) in $SrTiO_3$. The lowest-energy configurations for $nH–V_{Ti}$ complexes ($n=1$, 2, 3, 4) were identified and their vibrational frequencies were calculated. The calculated vibrational frequencies of $nH–V_{Ti}$ complexes are in the range of 2900–3400 cm^{-1}. For the complexes containing more than one O–H oscillator, there is some coupling between the stretch vibration modes. For $2H–V_{Ti}$ complex, the coupling leads to the split in the two vibration frequencies of 26 cm^{-1}. This combined with our previous study of $nH–V_{Sr}$complexes in $SrTiO_3$, indicates that the twin IR absorption peaks at 3355 and 3384 cm^{-1} observed by Tarun and McCluskey [14] are associated with the complex defects between H and V_{Ti}. On the other hand, the higher IR absorption peaks at $\sim$3500 cm^{-1}, observed much earlier by Weber and Kapphan, are associated with the complex defects between H and V_{Sr}.

Acknowledgements

Support from the Thailand Research Fund (Grant No. RTA5280009) and US Department of Energy, Division of Materials Sciences and Engineering are acknowledged. One of the authors (IF) acknowledges the scholarship from the Development and Promotion of Science and Technology Talents Project (DPST).

Reference

[1] M.-H. Du, K. Biswas, Anionic and hidden hydrogen in ZnO, Physical Review Letters 106 (2011) 115502.
[2] W.M. Hlaing, Oo, S. Tabatabaei, M.D. McCluskey, J.B. Varley, A. Janotti, C.G. Van de Walle, Hydrogen donors in SnO_2 studied by infrared spectroscopy and first-principles calculations, Physical Review B 82 (2010) 193201.
[3] P.D.C. King, R.L. Lichti, Y.G. Celebi, J.M. Gil, R.C. Vilão, H.V. Alberto, J. Piroto Duarte, D.J. Payne, R.G. Egdell, I. McKenzie, C.F. McConville, S.F.J. Cox, T.D. Veal, Shallow donor state of hydrogen in $In2O_3$ and SnO_2: implications for conductivity in transparent conducting oxides, Physical Review B 80 (2009) 081201.
[4] S. Limpijumnong, P. Reunchan, A. Janotti, C.G. Van de Walle, Hydrogen doping in indium oxide: an ab initio study, Physical Review B 80 (2009) 193202.
[5] Z. Kun, J. Kui-juan, H. Yanhong, Z. Songqing, L. Huibin, H. Meng, C. Zhenghao, Z. Yueliang, Y. Guozhen, Ultraviolet fast-response photoelectric effect in tilted orientation $SrTiO_3$ single crystals, Applied Physics Letters 89 (2006) 173507.
[6] G.M. Rao, S.B. Krupanidhi, Study of electrical properties of pulsed excimer laser deposited strontium titanate films, Journal of Applied Physics 75 (1994) 2604.
[7] N. Seung-Hee, K. Ho-Gi, The effect of heat treatment on the $SrTiO_3$ thin films prepared by radio frequency magnetron sputtering, Journal of Applied Physics 72 (1992) 2895.
[8] F.J. Walker, R.A. McKee, Y. Huan-wun, D.E. Zelmon, Optical clarity and waveguide performance of thin film perovskites on MgO, Applied Physics Letters 65 (1994) 1495.
[9] X.D. Wu, D. Dijkkamp, S.B. Ogale, A. Inam, E.W. Chase, P.F. Miceli, C.C. Chang, J.M. Tarascon, T. Venkatesan, Epitaxial ordering of oxide superconductor thin films on (100) $SrTiO_3$ prepared by pulsed laser evaporation, Applied Physics Letters 51 (1987) 861.
[10] D. Houde, Y. Lepine, C. Pepin, S. Jandl, J.L. Brebner, High-resolution infrared spectroscopy of hydrogen impurities in strontium titanate, Physical Review B 35 (1987) 4948.
[11] S. Kapphan, J. Koppitz, G. Weber, O–D and O–H stretching vibrations in monodomain $SrTiO_3$, Ferroelectrics 25 (1980) 585.
[12] G. Weber, S. Kapphan, M. Wohlecke, Spectroscopy of the O–H and O–D stretching vibrations in $SrTiO_3$ under applied electric field and uniaxial stress, Physical Review B 34 (1986) 8406.
[13] S. Klauer, M. Wohlecke, Local symmetry of hydrogen in cubic and tetragonal $SrTiO_3$ and $KTaO_3$: Li determined by polarized Raman scattering, Physical Review Letters 68 (1992) 3212.
[14] M.C. Tarun, M.D. McCluskey, Infrared absorption of hydrogen-related defects in strontium titanate, Journal of Applied Physics 109 (2011) 063706.
[15] J.T.- Thienprasert, I. Fongkaew, D.J. Singh, M.H. Du, S. Limpijumnong, Identification of hydrogen defects in $SrTiO_3$ by first-principles local vibration mode calculations, Physical Review B 85 (2012) 125205.
[16] G. Kresse, J. Furthmüller, Efficiency of ab-initio total energy calculations for metals and semiconductors using a plane-wave basis set, Computational Materials Science 6 (1996) 15.
[17] G. Kresse, J. Hafner, Norm-conserving and ultrasoft pseudopotentials for first-row and transition-elements, Journal of Physics: Condensed Matter 6 (1994) 8245.
[18] G. Kresse, D. Joubert, From ultrasoft pseudopotentials to the projector augmented-wave method, Physical Review B 59 (1999) 1758.
[19] F.W. Lytle, X-ray diffractometry of low-temperature phase transformations in strontium titanate, Journal of Applied Physics 35 (1964) 2212.
[20] C.G. Van de Walle, J. Neugebauer, First-principles calculations for defects and impurities: applications to III-nitrides, Journal of Applied Physics 95 (2004) 3851.
[21] R.P. Feynman, Forces in molecules, Physical Review 56 (1939) 340.
[22] H. Hesse, S. Kapphan, Doping of $SrTiO_3$ with hydrogen and deuterium, Physica Status Solidi A Applications and Material Science 50 (1978) K243.
[23] S. Daniel, T. Rye, H. Graeme, Optimization methods for finding minimum energy paths, Journal of Chemical Physics 128 (2008) 134106.
[24] H. Graeme, P.U. Blas, J. Hannes, A climbing image nudged elastic band method for finding saddle points and minimum energy paths, Journal of Chemical Physics 113 (2000) 9901.
[25] H. Graeme, J. Hannes, Improved tangent estimate in the nudged elastic band method for finding minimum energy paths and saddle points, Journal of Chemical Physics 113 (2000) 9978.
[26] G. Mills, H. Jonsson, G.K. Schenter, Reversible work transition state theory: application to dissociative adsorption of hydrogen, Surface Science 324 (1995) 305.
[27] J.T.- Thienprasert, S. Limpijumnong, A. Janotti, C.G. Van de Walle, L. Zhang, M.H. Du, D.J. Singh, Vibrational signatures of OTe and OTe-VCd in CdTe: a first-principles study, Computational Materials Science 49 (2010) S242.
[28] K.P. Huber, G. Herzberg, Molecular Spectra and Molecular Structure. IV. Constants of Diatomic Molecules, Van Nostrand Reinhold Co., 1979.
[29] T. Shimanouchi, Tables of Molecular Vibrational Frequencies, Consolidated Volume 1, NSRDS NBS-39.